Technical Implications of Neglecting Compositional Grading Effects in Petroleum Reservoir simulation Models

Ikechi Igwe[+], **Jebraeel Gholinezhad*[+], *Mohamed Galal Hassan Sayed*[++], *Frank Obuagu*[+++]

[+]School of Energy and Electronic Engineering, Anglesea Building, University of Portsmouth, Portsmouth, PO1 3DJ, United Kingdom.

[++]Chemical Engineering Building 30, University of Southampton, Southampton, SO17 IBJ, United Kingdom.

[+++]Chevron Nigeria Limited, Lagos, Nigeria.

Keywords: Compositional grading; reservoir modeling and simulation; reservoir performance; uncertainty assessment; response surface methodology.

Abstract

Most compositional reservoir simulation practices assumes that the compositions of various fluid components are the same at all locations within the reservoir system. This constant composition assumption is incorrect and unrealistic as it grossly ignores the occurrences of some less obvious physical processes in the reservoir. Gravitational force, temperature gradient and thermal diffusion, amongst other factors, contributes to distribution and gradation of hydrocarbon fluid compositions in the reservoir. Therefore, incorporating compositional grading models that

adequately accounted for the individual and combined effects of gravity force, temperature gradient, and thermal diffusion is crucial when initializing reservoir simulation models. This research seeks to elucidate the technical implications of compositional grading on improved reserve estimation and reservoir performance prediction. The mathematical framework for the compositional grading modeling is based on one-dimensional zero-mass-flow stationary state assumption. The Computer Modelling Group's equation of state multiphase equilibrium property simulator, WinProp, was used for the fluid modeling while Computer Modelling Group's compositional reservoir simulator, GEM, was used for the reservoir modeling and simulation. In the absence of historical production data, Computer Modelling Group's CMOST was used to perform uncertainty assessment for the validation of the initialized reservoir models. The research results show that initialized reservoir models that neglected or inadequately accounted for compositional grading effects, overestimated oil in-place and underestimated gas in-place. Constant composition (without compositional grading) initialized reservoir model overestimate ultimate cumulative oil production by 14.271 MMbbl more than the isothermal compositional grading model, and 24.088 MMbbl more than the Kempers thermal diffusion compositional grading initialized reservoir model. It underestimated ultimate cumulative gas production by 30.133 Bft^3 less than the isothermal compositional grading, and 50.408 Bft^3 less than the Kempers thermal diffusion compositional grading initialized reservoir model. These figures suggest that neglecting compositional grading or inadequate account of compositional grading effects in reservoir simulation initialization, has detrimental technical consequences.

1. INTRODUCTION

Hydrocarbon fluids consist of several hydrocarbon and non-hydrocarbon components, ranging from the light molecular weight components such as methane (C_1) to the heavy plus fractions.

The compositions of the various components in the oil and gas phases differs due to certain reservoir conditions (such as gravity and temperature). To efficiently produce petroleum reservoir fluids from the reservoir to the surface, it is necessary to know the components and compositions of the fluids, the behavior of the fluids at reservoir and surface conditions, respectively, and the processes and factors responsible for the established behavior of the fluid systems. These tasks could be achieved with the help of reservoir simulation study. A reservoir simulation model is a mathematical model which represents an actual reservoir such that the model simulates the actual behavior of the reservoir as much as possible.[1]

Most compositional reservoir simulation practices assumes that the compositions of the various fluid components are the same at all locations within the reservoir system. However, recent studies have shown that the constant composition assumption is incorrect and unrealistic as it grossly ignores the occurrences of some less obvious physical processes in some reservoirs. Gravitational force, temperature gradient, and thermal diffusion, amongst other factors, contributes significantly to distribution and gradation of hydrocarbon fluid compositions in the reservoir.[2–9] This compositional variation with depth is what is known as compositional grading (CG) or compositional gradient. CG in petroleum reservoirs will give rise to variation in other fluid properties, such as gas-oil ratio (GOR), saturation pressure, density, and molecular weight.[8-10] Therefore, to accurately estimate in-place volumes and reservoir performances, it is necessary to initialize applied reservoir simulation model with CG model that adequately accounts for the factors responsible for CG in the reservoir system.[11] The effect of gravity alone is simulated using the isothermal CG model while the combine effect of gravity, temperature gradient and thermal diffusion are simulated based on non-isothermal CG models – zero thermal diffusion model; Haase's thermal diffusion model; and Kemper's thermal diffusion model.

Available literature indicates limited application of CG models for reservoir model initialization, with isothermal CG model as the main CG model that has been applied for this purpose.[11–17] However, it has been shown that gravity effect alone and the constant temperature assumptions by isothermal CG model are grossly inappropriate since temperature gradient and its concomitant thermal diffusion effect also contribute to compositional variations with depth in the reservoir.[3,7,9,18] Limited reports of reservoir models initialized with CG models (non-isothermal CG models) that adequately accounts for the factors responsible for CG in hydrocarbon reservoirs, portend a substantial gap in knowledge. Therefore, by using CG models that adequately accounted for the individual and combined effects of gravity force, temperature gradient, and thermal diffusion effects to initialize reservoir simulation models, this research seek to elucidate the technical implications of CG on accurate reserve estimation and reservoir performances prediction.

2. MODELING METHODOLOGY

2.1. Compositional Grading Models

The modeling frameworks for the estimation of compositional variation with depth in petroleum reservoirs have been reported in the literature.[3,19–22] There are three main categories of these modeling frameworks.[3] The thermodynamic based models (static models), which relies on fluid enthalpies to estimate thermal diffusion coefficient.[3,9,23–30] The second category are based on activation energy (dynamic models), which is obtained from viscosity correlations.[29,31–33] The third category requires molecular diffusion coefficient and convection term.[29,33–41]

CG models in the above mentioned second and third categories were not considered in this study because they are not supported by the applied CMG's WinProp simulator. To include these models in this study would require developing separate solution algorithms for each of them,

which is beyond the scope of this study. The list of available non-isothermal CG models is rather extensive. This suggest why no single research effort has been able to apply all the various CG models.[22] For instance, Esposito et al.[29] presented CG simulation results based on non-isothermal models other than those applied in this work. The non-isothermal models applied by Espsito et al.[29] include Pederson and Linderloff[42] model, Pederson and Hjermstad[43] model, and Ghorayeb et al.[44] model. More so, in an exceptional case where some static and dynamic CG models have been applied by Høier and Whitson,[3], the authors were not directly responsible for the results obtained by the application of Firoozabadi-Ghorayeb[35] model. Høier and Whitson[3] reported that the result presented from application of Firoozabadi-Ghorayeb[35] model was provided by a third party. Høier and Whitson[3] also posited that for reservoir fluid similar to this study reservoir system, the CG model that accounted for kinetic contribution to compositional variation with depth (Firoozabadi-Ghorayeb[35] model), predicted similar CG as the static models applied in this study (Haase's model and Kempers model). Hence, the scope of this current study is limited to isothermal model, passive thermal diffusion model, Haase's model, and Kempers model, which are supported by the applied CMG's WinProp simulator.

The one-dimensional zero-mass-flow stationary state model assumptions applied in this work can be written for the combined effects of gravity and thermal diffusion effects thus:

$$\nabla \mu_i = Q_{Gi} - Q_{Ti} \frac{\nabla T}{T} \qquad (1)$$

In Eq. (1), μ_i is the chemical potential of component i, ∇T is the temperature gradient, T is the system temperature, h is the depth of interest, Q_{Gi} accounts for the effect of gravity, and Q_{Ti} denotes thermal diffusion factor. The term Q_{Gi} is expressed thus:

$$Q_{Gi} = \left(M_i - \rho V_i\right) g \tag{2}$$

where M_i is the molecular weight of component i, V_i is the partial molar volume of component i, ρ is mass density, and g is the acceleration due to gravity.

A major constraint to the application of Eq. (1) is that the sum of the mole fractions of all fluid components at a given depth along the hydrocarbon column must add up to one (unity). That is:

$$\sum_{i=1}^{n} z_i(h) = 1 \tag{3}$$

where n is the number of components and z_i is the overall composition of component i. Therefore, there are $n+1$ variables at any given depth along the hydrocarbon column. To predict the pressure and molar compositions at any depth will accordingly require resolving $n+1$ equations consisting $n+1$ variables, using applied EOS. Eq. (1) is the compositional grading model used in this work.

Isothermal CG model neglects the effect of thermal gradient and thermal diffusion (Q_{Ti}= 0) by assumes thermodynamic equilibrium conditions in the reservoir. Thus, gravity force is the only factor responsible for the distribution of fluid compositions in the reservoir, causing lighter components like methane to migrate towards the top of the reservoir and heavier components to move towards the bottom section. Eq. (1) can be precisely transformed to an isothermal model by expressing it in terms of component fugacity as follows:

$$f_i\left(h\right) = f_i\left(h^o\right) exp\left(-\frac{M_i g\left(h - h^o\right)}{RT}\right) \quad i = 1, 2\ldots, n \tag{4}$$

The fugacity of component i can be calculated based on the overall composition of the species, thus:

$$f_i = p_i z_i \varphi_i \tag{5}$$

Consequently, Eq. (4) can be rewritten as:

$$(\varphi_i^h z_i^h p_i^h) = (\varphi_i^{(h^o)} z_i^{(h^o)} p_i^{(h^o)}) exp\left(-\frac{M_i g\left(h - h^o\right)}{RT} \right) i = 1, 2, ..., n \tag{6}$$

Where, f_i is the fugacity of component i, h^o is the reference depth, h is the depth of interest, R is the acceleration due to gravity, p_i is the pressure of component i, φ_i is the fugacity coefficient of component i, and all other terms are as defined in Eq. (1). Eq. (6) is the isothermal CG model used in this work.

Petroleum reservoirs with a specific temperature gradient are regarded as non-isothermal reservoirs and will not be at thermodynamic equilibrium, hence, can only be modeled with non-isothermal models. Zero or passive thermal diffusion model is a hypothetical model in which the thermal diffusion factor (J_{Ti}) in Eq. 3.1 is assumed to be negligible even though thermal gradient exist in the system ((J_{Ti}) = 0, $\nabla T \neq 0$). The temperature, T at a depth, h was estimated from the knowledge of temperature gradient (∇T). By assuming (J_{Ti}) = 0 but accounting for thermal gradient, Eq. 1 was solved by integrating with depth discretization using applied computer simulator (CMG *WinProp*).

Haase's thermal diffusion model estimates thermal diffusion coefficient based on the centre of mass assumption as follows:

$$Q_{Ti} = \frac{1}{M_i} . \left(M_i H_m - M_m H_i \right) \tag{7}$$

Where

$$M_m = \sum_i x_i M_i \tag{8}$$

$$H_m = \sum_i x_i H_i \tag{9}$$

M_m is the molecular weight of the mixture, H_m is the molar enthalpy of the mixture, M_i is the molecular weight of component i in the mixture, H_i is the partial molar enthalpy of component i in the mixture, x_i is the mole fraction of component i.

Kempers thermal diffusion model calculates thermal diffusion coefficient (factor) based on centre of volume assumption as follows:

$$Q_{Ti} = \frac{1}{V_i}.\left(V_i H_m - V_m H_i\right) \tag{10}$$

where

$$V_m = \sum_i x_i V_i \tag{11}$$

V_m is the molar volume of the mixture, V_i is the partial molar volume of component i in the mixture.

2.2. Reservoir Fluid Characterization

Fluid data of a high shrinkage black oil reservoir fluid sample (41.9 ^{o}API) obtained at a reference depth of 7655 ft and used for this work, is presented in Table 1. The sample (fluid data) was characterized based on Peng-Robinson equation of state (EOS) with the 1978 expression for the constant "α" (a function introduced to fit the vapor pressure data of petroleum mixture), using *WinProp*. *WinProp* is the Computer Modeling Group's (CMG's) EOS multiphase equilibrium

property simulator. The applied EOS was selected based on the work of Igwe et al.[22] The characterization process starts with the selection of the EOS, specification of unit and feed (mole or mass). The heptane plus fraction was defined using the molecular weight and specific gravity. Critical temperature and pressure, acentric factor, and molecular weight of the heptane plus fraction were selected for the tuning of the EOS fluid model. This is to ensure accurate prediction of saturation pressure and vapor-liquid equilibrium estimation. The regression procedure presented by Agarwal et al,[45] is what *WinProp* uses to tune the EOS models. This procedure ensures that the most sensitive parameter amongst selected parameters is regressed first. The flowchart for CG modeling and simulation based on CMG WinProp is presented in Figure 1. Table 2 shows that five (5) fluid models were built and used for initialization of the reservoir simulation models.

Table 1. Reservoir Fluid Composition and Properties at Reference Depth of 7655 ft.

Component	**Mole fraction**
CO_2	0.0143
C_1	0.4608
C_2	0.0518
C_3	0.0648
iC_4	0.0211
nC_4	0.0354
iC_5	0.0194
nC_5	0.0195
C_6	0.038
C_{7+}	0.2749
C_{7+} Molecular weight (g/mol)	200
C_{7+} specific gravity	0.8347
Saturation pressure (psia)	3391.64
Reservoir pressure (psia)	3487
Reservoir temperature (^oF)	230
Depth to top of sand (ft)	7398
Depth to bottom of sand (ft)	7996

Table 2. Fluid Models used in Initializing the Reservoir Models

Fluid Models	Description
Constant Composition	Without CG
Isothermal CG	Constant Temperature
Zero Thermal Diffusion CG	Non-isothermal
Haase's	Non-isothermal CG
Kempers	Non-isothermal CG

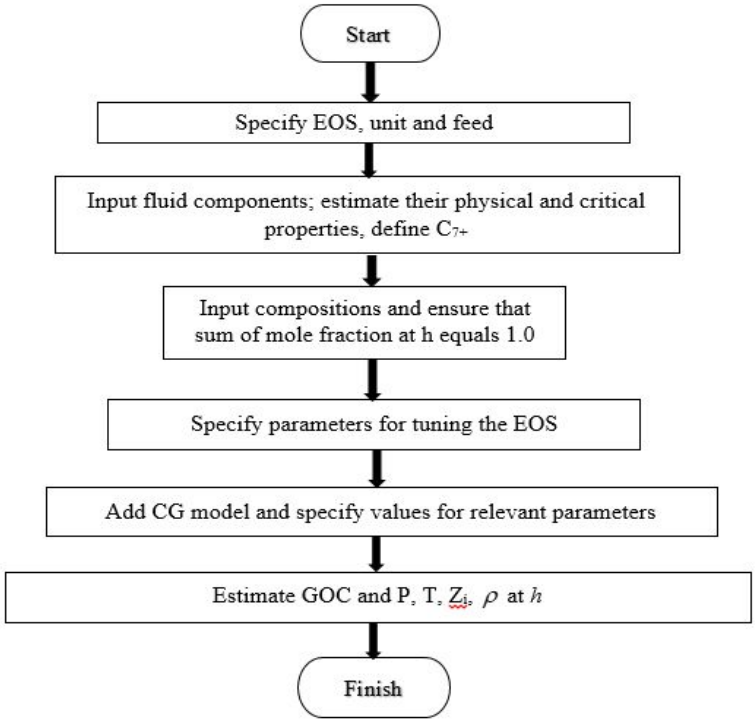

Figure 1. Flowchart of CG Modeling Steps Using WinProp

2.3. Geomodeling

CMG Builder was used for the building of the geologic model. The reservoir simulator setting was specified by selecting the simulator type (in this case, GEM), working unit (field), and porosity (single porosity). The simulation start date was also specified. Builder static model task manager was used in creating the geologic model. Three major steps were involved. The first step involves importing the well trajectories, well logs, and formation tops. Geological maps or horizons were created in the next step. Top and bottom maps associated with the top and bottom markers, respectively, were created based on the invers distance estimation method. A 2D corner-point-grid system was created for one geologic unit and the dimensions presented in Table 3. Ten (10) vertical layers were added to the 2D grid to create the 3D grid model. The last step in building the geologic model involves assigning the created contour maps to the built 3D grid model, thereby generating the actual reservoir topology presented in Figure 2, which is the geologic (static) model of the study reservoir with 26 x 54 x 10 gridblocks (14040 gridcells).

Table 3. Grid System Dimensions

Parameter	Value
Origin X	836538
Origin Y	633816
Rotation	0
Size X	3900
Size Y	6480
Delta X	150
Delta Y	120
NX	26
NY	54
No. of cells per layer	1404

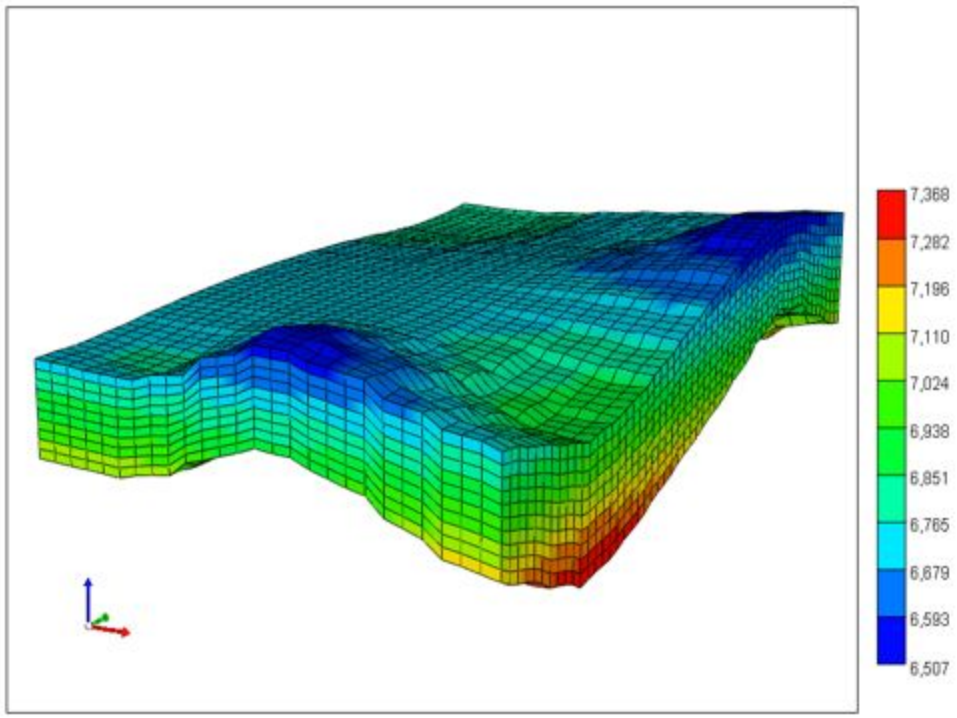

Figure 2. 3D Geologic Model of the Study Reservoir

2.4. Dynamic Reservoir Modeling Procedure

The study reservoir geologic model was converted to a dynamic reservoir model by populating the gridblocks with dynamic data. There was no need for upscaling since the geomodel was constructed with few thousand grid blocks that sufficiently represent the actual reservoir and satisfied the study objective. The objective of the reservoir simulation study is to build reservoir flow models for the investigation of the technical implications of initializing reservoir simulation model with various CG models. A corner point grid system representing a sector model of the study reservoir with 14,040 grid cells and the available geological, geophysical, and engineering data were sufficient for this purpose. The values of reservoir properties provided in Table 4 were specified in the array property node of the reservoir model. Permeability distribution (Permeability I and permeability J) was based on Gaussian geostatistical simulation and ranges from 52–125 mD. Gaussian geostatistical-simulation accounts for the uncertainty associated with

some reservoir properties (permeability and porosity). Permeability K was set equals permeability I*0.1. Rock compressibility of $3.0*10^{-06}$ psi^{-1} was also specified. The reservoir porosity ranges from 0.16–0.25, with an average porosity of 0.205.

There was no aquifer definition or support for the study reservoir and report from the industry indicates that the reservoir was placed under water injection pressure-maintenance from initial production period. The coupling of the CG models (PVT models) into the reservoir model was implemented in the component section of Builder tree view. The fluid models built in section 2.2 and listed in Table 2 were coupled individually with the reservoir model. Therefore, five (5) initialized dynamic reservoir models were built – constant composition, isothermal CG, Zero thermal diffusion CG, Haase's thermal diffusion CG, and Kempers thermal diffusion CG initialized reservoir models, respectively. The composition of each component as they vary with depth were specified for the various reservoir models. The reservoir gridblock temperature with respect to depth were also specified for the non-isothermal CG initialized models. The oil-water and gas-oil relative permeability presented in Figures 3 and 4, respectively, were specified. Specified oil-water capillary pressure is shown in Figure 5. The simulator recommended separator conditions for calculation of initial fluid-in-place was also specified.

Six (6) wells were defined and completed, four producers and two water injection wells. Two operating well constraints were set for the four (4) producers. The first is a maximum surface oil rate (STO) and secondly, a minimum bottom hole pressure (BHP). The values of the constraints for each producer well are presented in Table 5. Well-6 and well-7 were defined as injectors. A maximum bottom hole pressure (BHP) of 4100 psi and surface water rate (STW) of 15170 bbl/day were set as the first and second operating constraints, respectively, for Well-6 while a maximum BHP of 4100 psi and STW of 5170 bbl/day were set as the first and second operating

constraints, respectively, for Well-7. The well locations and completions are indicated in Figure 6. The models were then executed and simulation results analyzed and recorded.

Table 4. Study Reservoir Parameters

Parameter	**Value**
Permeability , mD	52-125
Porosity, fraction	0.16-0.25
Vertical/Horizontal Permeability Ratio	0.1
Rock Compressibility, psia-1 @ 3000 psia	0.000003
Initial Reservoir Pressure, psia	3487
Initial Reservoir Temperature, ^{o}F	230

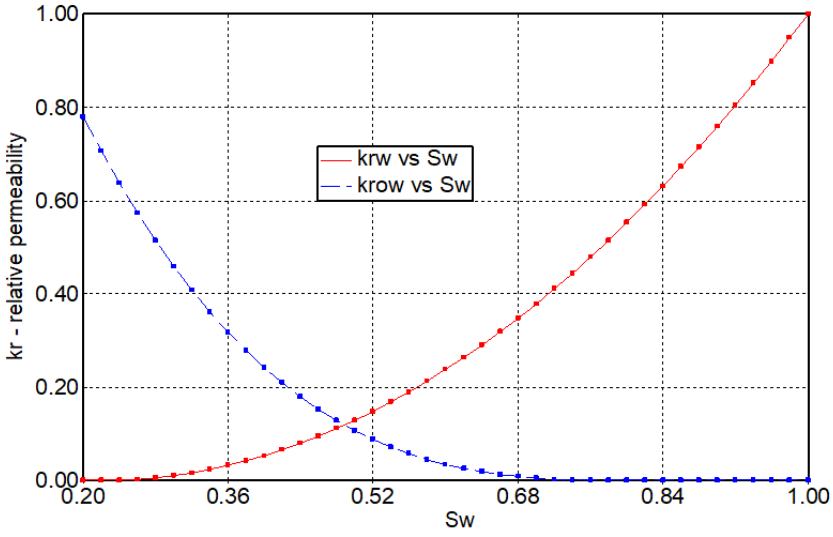

Figure 3. Oil-Water Relative Permeability Curve

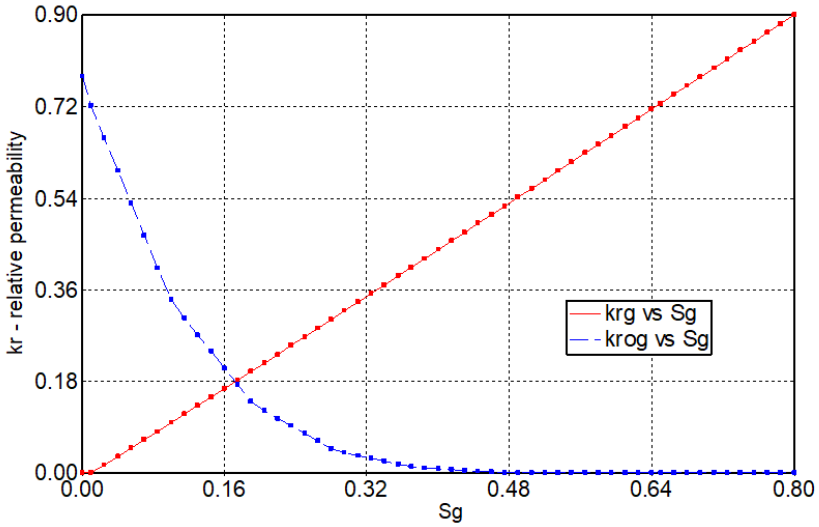

Figure 4. Gas-Oil Relative Permeability Curve

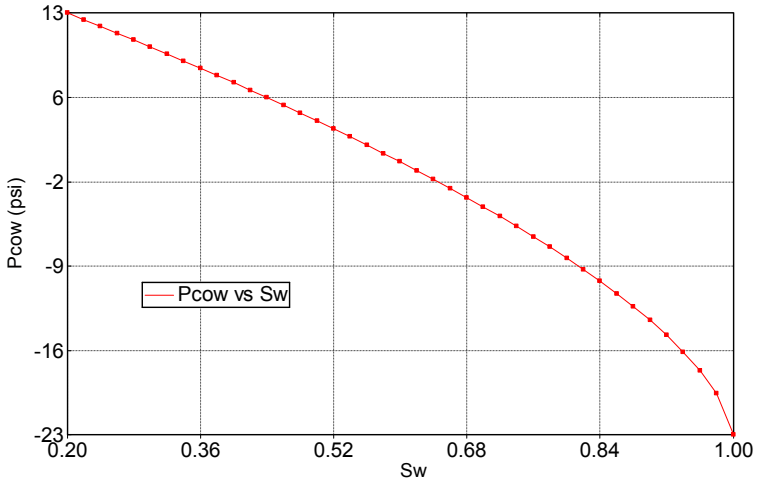

Figure 5. Capillary Pressure Curve

Table 5. Well Events and Constraints

S/No	Constraint	Limit	Well-4	Well-5	Well-6	Well-7	Well-8	Well-9
1	STO (bbl/day)	Maximum	3619	2019	Injector*	Injector*	2019	2019
2	BHP (psi)	Minimum	2500	2000	Injector*	Injector*	2000	2000

**Injector values are specified in section 2.4.*

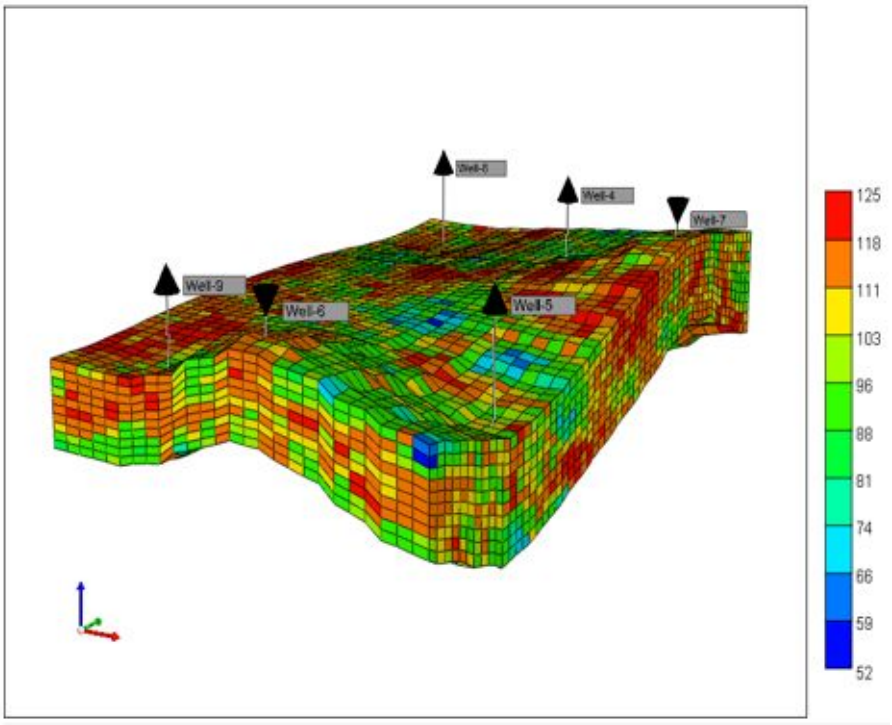

Figure 6. Well Locations and Completion in the Reservoir Model

2.5. Model Validation

The following methods were used in validating the various initialized reservoir model results:

i. Comparison of the deterministic reserve estimate (reservoir simulation estimate) to the probabilistic reserve estimate. The reservoir simulation result is said to be valid if both deterministic and probabilistic estimates agree significantly. If both estimates differ dramatically, the reservoir model assumptions will have to be reconsidered.[46,47]

ii. By quantifying the uncertainty in the estimated in-place volumes using Monte Carlo Simulation (MCS).[3]

iii. Response surface methodology – by plotting the simulated in-place volume against proxy model (MCS) predicted in-place volumes (response surface model verification plot or model quality check plot), the validity or otherwise of the initialized reservoir models can be established. The model quality-check plot indicates how meticulously the proxy model

predictions match actual reservoir simulation results. The 45-degree line indicate a perfect match between the proxy model and actual reservoir simulation responses. The closeness of the experiments to the 45-degree line shows how perfectly the proxy model matched the reservoir simulation results. The points that are exactly on the 45-degree line are those that are predicted perfectly. The farther away a point is from the 45-degree line, the more its outlier. The indicated training experiments are used by CMOST to create the proxy model while the verification experiments are used to check if the created proxy model is a valid proxy to the actual reservoir simulation responses.[48] Reduced Quadratic regression model was used to determine whether the regression model is statistically significant. The model is said to be statistically significant at 5 % probability if the 95 % confidence curves cross the horizontal reference line defined by the mean of response.[49]

iv. Experimental design quality of the regression model – the orthogonality of the experimental design gives an indication of the validity of the model. A CMOST regression model is assumed valid if the orthogonality of the experimental design quality is within the range of 0–0.2.[48]

2.6. Uncertainty Assessment (AU)

According to Høier and Whitson,[3] when field data are unavailable for history matching, the one-dimensional zero-mas-flux stationary state CG initialized reservoir models can be validated by using "cases" to quantify the range of uncertainties in the estimated in-place quantities. In addition, it has been shown that, if the deterministically (in this case, CG initialized reservoir model) estimated in-place volumes and the probabilistic values agree significantly, there is an increased confidence in the reserves estimation, thereby validating the model. If the two values differ dramatically, the reservoir model assumptions would need to be reconsidered.[46,47] Hence, the uncertainty associated with the CG initialized reservoir models reserve estimates were assessed using CMOST, a CMG software which relies on CMG reservoir simulators to perform

UA. CMOST also rely on response surface methodology to build proxy models that was used for further validation of the reservoir models. Input data such as fundamental time series (initial oil and gas volumes), regression variables (such as porosity, water saturation, and pay thickness), and objective functions (oil and gas in-place volumes), were imported into CMOST from CMG Builder base dataset. UA was performed based on Monte Carlo Simulation (MCS) using reservoir simulator.

The range of uncertainties in the estimated in-place volumes for the various initialized reservoir models were illustrated with non-exceedance cumulative probability distribution curves thus:

- P10 – there is at least 10 % probability that the volumes actually recovered will be less than the low estimate. This is equivalent to P90 of the probability of exceedance curve
- P50 – there is at least 50 % probability that the volumes actually recovered will be less than or equal the best estimate
- P90 - there is at least 90 % probability that the volumes actually recovered will be less than the high estimate. This is equivalent to P10 of the probability of exceedance curve

3. RESULTS AND DISCUSSION

3.1. CG simulation

Reservoir and Saturation Pressure Gradients. The trend of the reservoir pressure gradients predicted by the four CG models (isothermal, Zero thermal, Haase's, and Kempers) are presented in Figure 7, which demonstrates that within the gas zone, the reservoir pressure gradient predicted by various models varies marginally. However, there was no major difference in the reservoir pressure gradient predicted by the various models within the oil zone. Within the gas zone, Haase's thermal diffusion model predicted the lowest reservoir pressure gradient while the zero thermal diffusion and isothermal models, respectively, simulated the highest. The trend of reservoir pressure gradient predicted by the Kempers model was in between those predicted by Haase's model and zero thermal diffusion model.

Figure 8 presents the saturation pressure gradients predicted by the various CG models. Kempers model, zero thermal diffusion model, and isothermal model exhibited similar trends within the gas zone but with distinguishable GOCs. Isothermal model simulated higher saturation pressure gradient within the top gas zone and the bottom oil zone while Haase's thermal diffusion model predicted the least saturation pressure gradient in both zones. Figure 8 indicates that models which accounted for the combined effects of gravity and thermal diffusion (Haase model and Kemper's model) predicted lower saturation pressure gradients in the entire hydrocarbon column, due to the effect of thermal diffusion, which counteracts gravity effect. Figure 8 also show that without the effect of thermal diffusion, temperature gradient alone as hypothetically assumed in zero thermal diffusion model, only caused a marginal difference in saturation pressure gradient when compared to isothermal model prediction. Another relevant observation from Figure 8 is the difference in the saturation pressure gradients predicted by Haase's and Kempers models, respectively. This difference could be attributed to their methods of estimating thermal diffusion factor.

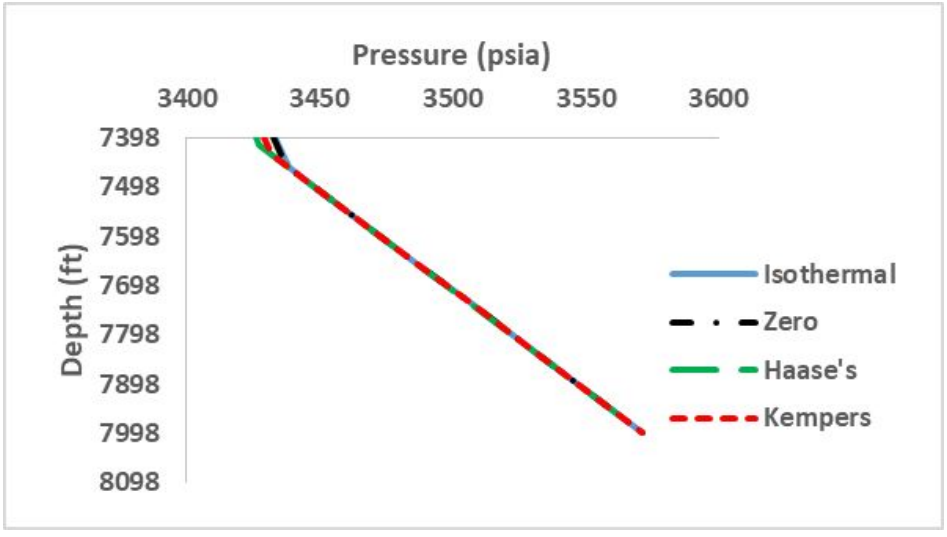

Figure 7. Reservoir Pressure Gradients Predicted by the Various CG Models

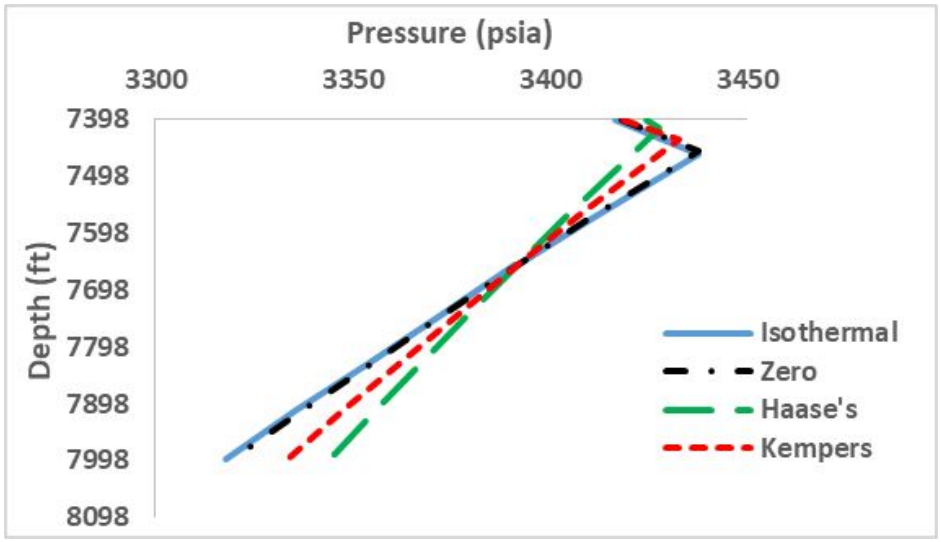

Figure 8. Saturation Pressure Gradients Predicted by the Various CG Models

Methane and Heptane plus fraction Gradients. Figures 9 and 10 presents the trends of C_1 and C_{7+} mole fraction variation with depth, respectively, simulated by the various CG models. The isothermal CG model predicted a suggestively sharp drop in C_1 mole fraction from the top of the hydrocarbon column to the GOC and then a gradual decrease with increasing depth up to the bottom of the column, which suggests that the reservoir oil is not very susceptible to CG. Zero thermal diffusion CG, Haase's thermal diffusion CG, and Kempers thermal diffusion CG models, respectively, indicated very marginal drop in C_1 mole fraction within the predicted gas zones followed by a sharp drop from the various GOC to the depth of 7483.43 ft. The variation in C_1 mole fraction after this depth is quite marginal and gradual with increasing depth. In addition, there is no major difference in C_1 gradation predicted by the various models after this depth (7483.43 ft) and up to the bottom of the hydrocarbon column. Figure 9 shows that C_1 mole fraction decreases with increasing depth, which is in agreement with trends reported in the literature.[3,7,9,18–22]

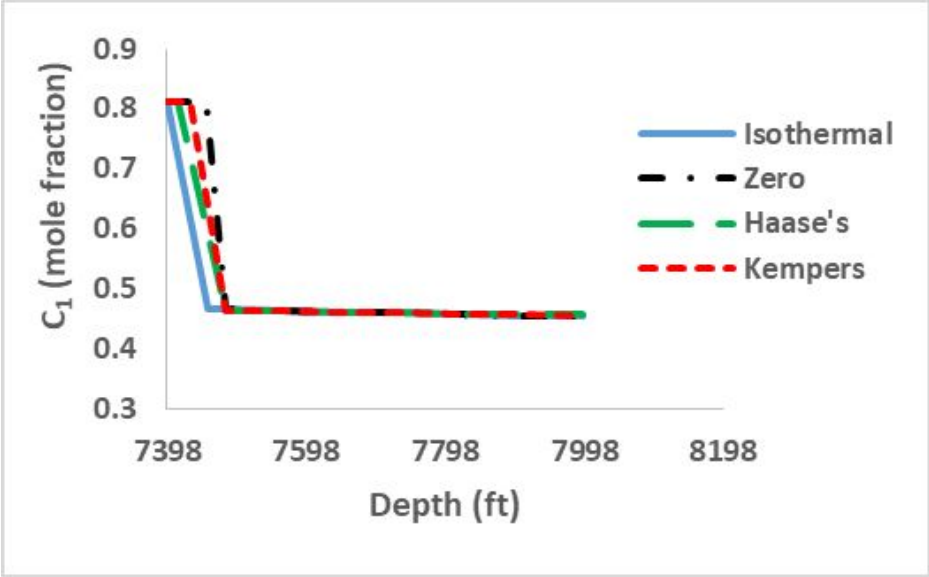

Figure 9. C_1 Mole Fraction Variation with Depth Predicted by the Various CG Models

Figure 10 indicates that C_{7+} mole fraction increased with depth, which is also in agreement with trends reported in the literature.[3,7,9,18–22] The isothermal CG model predicted a noteworthy sharp increase in C_{7+} mole fraction from the top of the hydrocarbon column to the GOC and then a gradual increase with increasing depth up to the bottom of the column. Zero thermal diffusion CG, Haase's thermal diffusion CG, and Kempers thermal diffusion CG models, respectively, indicated very marginal increase in C_{7+} mole fraction within the predicted gas zones followed by a sharp increase from the various GOCs to the depth of 7483.43 ft. The variation in C_{7+} mole fraction after this depth is quite marginal and gradual with increasing depth. Similar to C_1 gradation, there is no major difference in C_{7+} gradation predicted by the various models after this depth (7483.43 ft) and up to the bottom of the hydrocarbon column.

Figure 9 and 10 also shows that a temperature gradient of 0.002 ^{o}F/ft was enough to produce thermal diffusion effect that caused noteworthy compositional gradient, especially within the gas zone. The significant or insignificant effects of these marginal differences in CG predicted by the various models, would be illustrated in the reservoir simulation results. The compositional

variation with depth for other fluid components as predicted by the various CG models are presented in Tables 6–9.

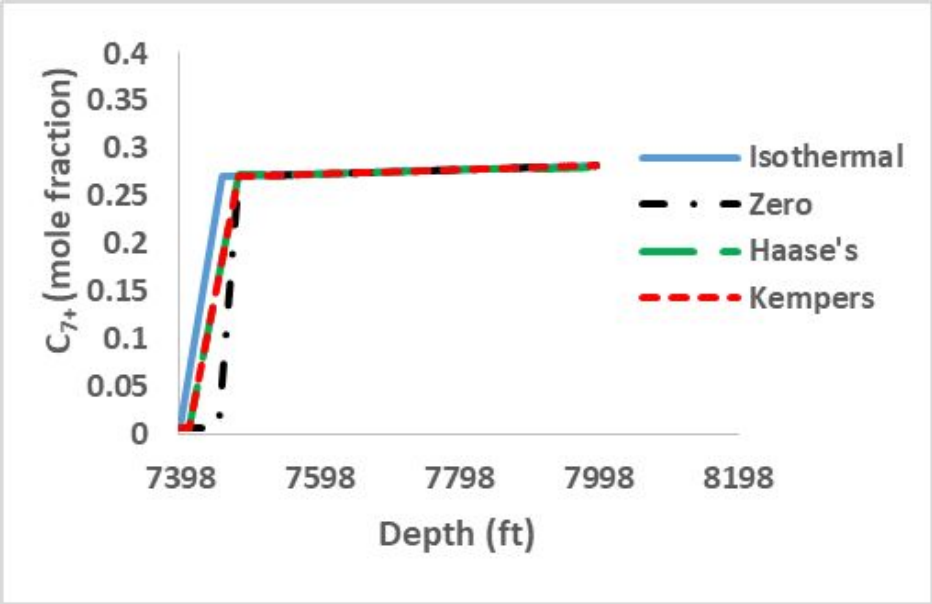

Figure 10. C_{7+} Mole Fraction Variation with Depth Predicted by the Various CG Models

The observed difference in CG between the fluid system within the top cold section of the reservoir and the bottom hot section can be attributed to the high sensitivity of the fluid system within the gas cap to gravity and thermal diffusion effects relative the fluid system towards the bottom hot section of the reservoir. The indicated small composition gradient in the oil zone and relatively large ones in the gas cap are similar to the trends reported by Igwe et al.[22] and Perdersen and Hjermstad.[11] Note that some literature have reported that different reservoir fluid systems behave differently with respect to compositional variation with depth.[9,11]

Table 6. Compositional Variation with Depth Predicted by Isothermal CG model

Depth (ft)	Composition (fraction)									
	CO2	C1	C2	C3	iC4	nC4	iC5	nC5	C6	C7+
7398.0	0.0144	0.8125	0.0568	0.0503	0.0128	0.0194	0.0083	0.0078	0.0112	0.0065
7458.1	0.0143	0.4654	0.0521	0.0650	0.0211	0.0354	0.0194	0.0195	0.0378	0.2699
7483.3	0.0143	0.4648	0.0521	0.0650	0.0211	0.0354	0.0194	0.0195	0.0379	0.2706
7568.9	0.0143	0.4628	0.0519	0.0649	0.0211	0.0354	0.0194	0.0195	0.0379	0.2727
7654.3	0.0143	0.4608	0.0518	0.0648	0.0211	0.0354	0.0194	0.0195	0.0380	0.2749
7655.0	0.0143	0.4608	0.0518	0.0648	0.0211	0.0354	0.0194	0.0195	0.0380	0.2749
7739.7	0.0143	0.4589	0.0517	0.0647	0.0211	0.0354	0.0194	0.0195	0.0381	0.2770
7825.1	0.0143	0.4570	0.0515	0.0646	0.0211	0.0354	0.0194	0.0195	0.0381	0.2790
7910.6	0.0143	0.4552	0.0514	0.0645	0.0211	0.0353	0.0194	0.0195	0.0382	0.2810
7996.0	0.0143	0.4534	0.0513	0.0644	0.0210	0.0353	0.0194	0.0195	0.0383	0.2830

Table 7. Compositional Variation with Depth Predicted by Zero Thermal Diffusion CG model

Depth (ft)	Temp. °F	Composition (fraction)									
		CO2	C1	C2	C3	iC4	nC4	iC5	nC5	C6	C7+
7398.0	229.5	0.0144	0.8126	0.0568	0.0502	0.0128	0.0194	0.0083	0.0078	0.0112	0.0065
7453.4	229.6	0.0144	0.8118	0.0569	0.0504	0.0129	0.0195	0.0083	0.0078	0.0113	0.0066
7483.4	229.7	0.0143	0.4648	0.0521	0.0650	0.0211	0.0354	0.0194	0.0195	0.0379	0.2706
7568.9	229.8	0.0143	0.4628	0.0519	0.0649	0.0211	0.0354	0.0194	0.0195	0.0379	0.2727
7654.3	230.0	0.0143	0.4608	0.0518	0.0648	0.0211	0.0354	0.0194	0.0195	0.0380	0.2749
7655.0	230.0	0.0143	0.4608	0.0518	0.0648	0.0211	0.0354	0.0194	0.0195	0.0380	0.2749
7739.7	230.2	0.0143	0.4589	0.0517	0.0647	0.0211	0.0354	0.0194	0.0195	0.0381	0.2770
7825.1	230.3	0.0143	0.4570	0.0515	0.0646	0.0211	0.0354	0.0194	0.0195	0.0381	0.2790
7910.6	230.5	0.0143	0.4552	0.0514	0.0645	0.0211	0.0353	0.0194	0.0195	0.0382	0.2810
7996.0	230.7	0.0143	0.4534	0.0513	0.0644	0.0210	0.0353	0.0194	0.0195	0.0383	0.2830

Table 8. Compositional Variation with Depth Predicted by Haase's Thermal Diffusion CG model

Depth	Temp.	Composition (fraction)									
(ft)	°F	CO2	C1	C2	C3	iC4	nC4	iC5	nC5	C6	C7+
7398.0	229.5	0.0145	0.8123	0.0569	0.0503	0.0128	0.0194	0.0083	0.0078	0.0113	0.0065
7412.9	229.6	0.0145	0.8122	0.0569	0.0503	0.0128	0.0194	0.0083	0.0078	0.0113	0.0066
7483.4	229.7	0.0143	0.4634	0.0520	0.0649	0.0211	0.0354	0.0194	0.0195	0.0379	0.2721
7568.9	229.8	0.0143	0.4621	0.0519	0.0649	0.0211	0.0354	0.0194	0.0195	0.0380	0.2735
7654.3	230.0	0.0143	0.4608	0.0518	0.0648	0.0211	0.0354	0.0194	0.0195	0.0380	0.2749
7655.0	230.0	0.0143	0.4608	0.0518	0.0648	0.0211	0.0354	0.0194	0.0195	0.0380	0.2749
7739.7	203.2	0.0143	0.4595	0.0517	0.0647	0.0211	0.0354	0.0194	0.0195	0.0380	0.2763
7825.1	230.3	0.0143	0.4583	0.0516	0.0647	0.0211	0.0354	0.0194	0.0195	0.0381	0.2776
7910.6	230.5	0.0143	0.4571	0.0515	0.0646	0.0211	0.0354	0.0194	0.0195	0.0381	0.2789
7996.0	230.7	0.0143	0.4559	0.0514	0.0645	0.0211	0.0354	0.0194	0.0195	0.0382	0.2802

Table 9. Compositional Variation with Depth Predicted by Kempers Thermal Diffusion CG model

Depth	Temp.	Composition (fraction)									
(ft)	°F	CO2	C1	C2	C3	iC4	nC4	iC5	nC5	C6	C7+
7398.0	229.5	0.0144	0.8125	0.0568	0.0503	0.0128	0.0194	0.0083	0.0077	0.0112	0.0065
7412.9	229.6	0.0144	0.8120	0.0569	0.0504	0.0129	0.0195	0.0083	0.0078	0.0113	0.0066
7483.4	229.7	0.0143	0.4640	0.0520	0.0650	0.0211	0.0354	0.0194	0.0195	0.0379	0.2714
7568.9	229.8	0.0143	0.4624	0.0519	0.0649	0.0211	0.0354	0.0194	0.0195	0.0379	0.2732
7654.3	230.0	0.0143	0.4608	0.0518	0.0648	0.0211	0.0354	0.0194	0.0195	0.0380	0.2749
7655.0	230.0	0.0143	0.4608	0.0518	0.0648	0.0211	0.0354	0.0194	0.0195	0.0380	0.2749
7739.7	203.2	0.0143	0.4593	0.0517	0.0647	0.0211	0.0354	0.0194	0.0195	0.0381	0.2766
7825.1	230.3	0.0143	0.4578	0.0516	0.0646	0.0211	0.0354	0.0194	0.0195	0.0381	0.2782
7910.6	230.5	0.0143	0.4563	0.0515	0.0646	0.0211	0.0354	0.0194	0.0196	0.0382	0.2798
7996.0	230.7	0.0143	0.4548	0.0514	0.0645	0.0211	0.0354	0.0195	0.0196	0.0382	0.2814

Gas-Oil Contacts. Figure 11 compares the GOCs predicted by the various CG models. This figure once again illustrates the effects of gravity and thermal diffusion on compositional grading modeling. The effect of the marginal difference between the saturation pressure gradients predicted by isothermal CG model and zero thermal diffusion CG model, which was due to gravity and temperature gradient effects (Figure 8) is a bit more amplified here. Gravity effect resulted to estimation of high GOC value by the isothermal model. A temperature gradient of 0.002 ^{o}F/ft without thermal diffusion did not significantly oppose the effect of gravity, hence, resulting in a marginal reduction in the GOC predicted by zero thermal diffusion CG model when compared to isothermal CG model. The noteworthy reduction in the GOCs predicted by Haase's and Kempers thermal diffusion models is an indication that thermal diffusion counteracts the effect of gravity. Therefore, the combined effect of gravity and thermal diffusion in CG models will inevitably produce more realistic simulation results that would adequately describe compositional grading phenomena in petroleum reservoirs.

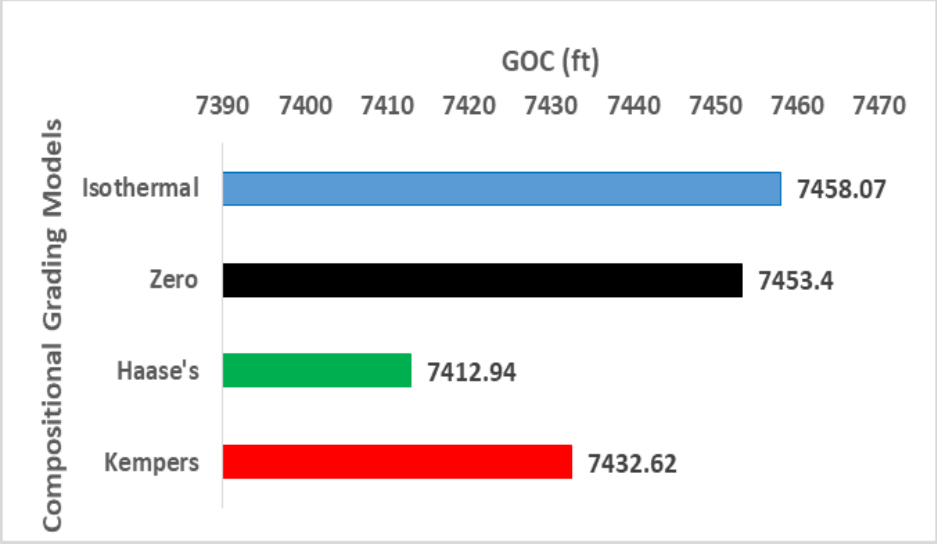

Figure 11. Comparison of GOCs Predicted by the Various CG Models

3.2. Reservoir Simulation

The simulation results of reservoir models initialized with constant composition fluid model, isothermal CG model, zero (passive) thermal diffusion CG model, Haase's thermal diffusion CG model, and Kempers thermal diffusion CG model, under water injection, are hereby presented and discussed. The only difference in the various initialized reservoir models is the PVT models or compositional grading models. All other parameters within the various initialized reservoir models are the same. This was intended for adequate comparison of the technical implications of the coupled CG models or constant composition PVT fluid model on the performances of resultant reservoir flow models. In the isothermal simulation, the initialized reservoir temperature does not change with time and locations. However, in the non-isothermal simulations, the initialized reservoir temperature changes with locations (depth) due to applied temperature gradient but remains constant with time. These are contrary to thermal simulators where the initialized reservoir temperature varies with both time and locations due to external heat sources, such as steam injection, in-situ combustion, and microwave heating. Technical performance indicators considered are the oil and gas production rates, reserve estimates, cumulative oil and gas production, gas-oil ratio, and average reservoir pressure profile. These technical performance indicators will illustrate the implications of implementing the various CG models in reservoir simulation model initialization.

Reserve Estimates. The oil originally in-place (OOIP) and gas originally in-place (GOIP) estimated by the various initialized reservoir models are presented in Figures 12 and 13, respectively. Figure 12 indicate that the reservoir model initialized without CG (constant composition fluid model) estimated the highest OOIP while Haase's thermal diffusion CG initialized reservoir model estimated the least OOIP. Although, isothermal CG initialized

reservoir model estimated OOIP lower than the value predicted by constant composition initialized reservoir model, the value is higher than the OOIP estimated by the various non-isothermal CG initialized reservoir models. There are marginal differences in the OOIPs predicted by the various non-isothermal initialized reservoir models.

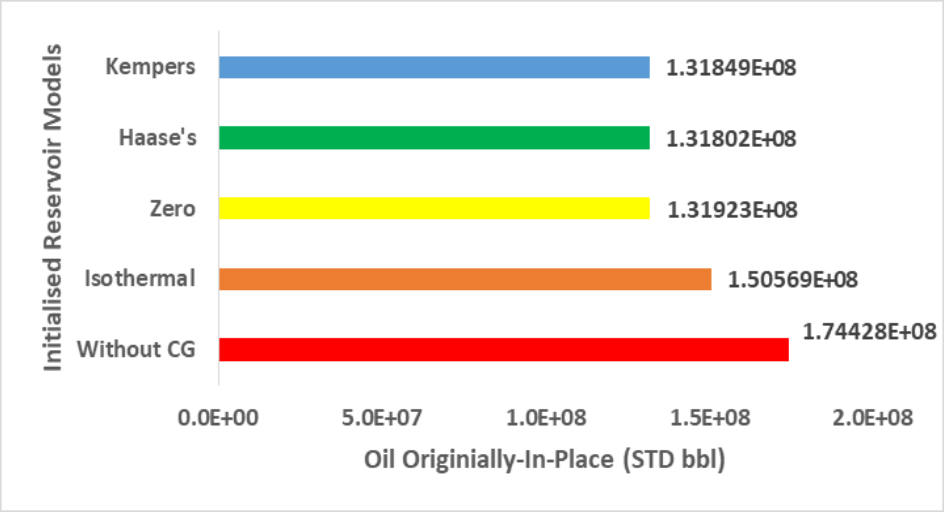

Figure 12. Oil Reserve Estimated by Various Initialized Reservoir Models

Figure 12 suggest that neglecting CG in reservoir model initialization and assuming that the compositions of the various reservoir fluid components is the same at any depth along the hydrocarbon column, resulted in high OOIP estimation. This assumption is not tenable, since this work have shown that the compositions of the various fluid components varies with depth. Hence, the constant composition (without CG) initialized reservoir model inevitably overestimated the OOIP. Figure 12 also shows that isothermal CG initialized reservoir model which neglected thermal diffusion effect also overestimated the OOIP. Similarly, isothermal assumption, with respect to the study reservoir, is not realistic, since this work has shown that thermal diffusion contributes to compositional gradation in the study reservoir. The zero thermal diffusion CG initialized reservoir model that accounted for both gravity and temperature gradient effects but neglected thermal diffusion effect, estimated marginally higher OOIP than the other

non-isothermal models (Haase's and Kempers CG initialized reservoir models). Since it is a hypothetical model, the result is also hypothetical. It can be opined from the forgoing analysis that Haase's and Kempers thermal diffusion initialized reservoir models, which accounted for the combined effect of gravity and thermal diffusion forces estimated the most realistic OOIP since they complied with physical realities (accounting for the effects of gravity and thermal diffusion).

It is evident from Figure 13 that constant composition initialized reservoir model estimated the lowest GOIP with respect to other models. This indicates that, following the previous analogy concerning OOIP, constant composition initialized reservoir model underestimated the GOIP. Again, this suggest that neglecting compositional grading in the initialization of reservoir simulation will result in underestimation of GOIP. Figure 13 also show that isothermal CG initialized reservoir model estimated higher GOIP than the constant composition initialized reservoir model. However, it estimated a low GOIP than the values indicated by the non-isothermal CG initialized reservoir models. Similarly, following previous analogy with respect to OOIP, neglecting the effects of thermal diffusion and temperature gradient as indicated by the isothermal CG initialized reservoir model will result in underestimation of GOIP. Figure 13 also indicates that zero thermal diffusion CG initialized reservoir model, which hypothetically accounted for the effect of temperature gradient but with passive thermal diffusion effect, estimated GOIP value higher than the values indicated by constant composition and isothermal CG initialized reservoir models but marginally lower than the values indicated by other non-isothermal models. Haase's and Kempers thermal diffusion CG initialized reservoir models estimated the highest GOIP with the value indicated by Haase's model marginally higher than the value predicted by Kempers initialized reservoir model.

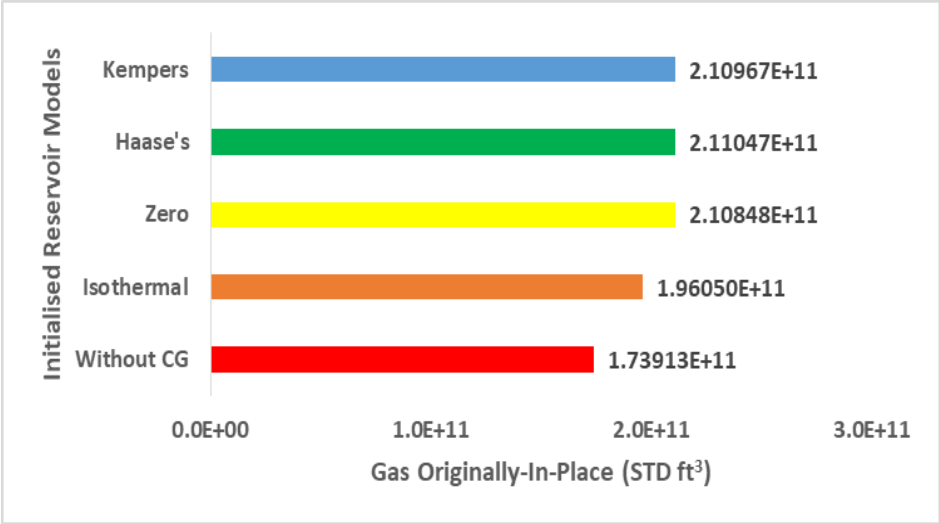

Figure 13. Gas Reserve Estimated by Various Initialized Reservoir Models

These results suggest that constant composition (without CG) initialized reservoir model overestimate the OOIP with 23.859 MMbbl more than the isothermal model, 42.505 MMbbl more than the zero thermal CG model, 42.626 MMbbl more than the Haase's thermal diffusion CG model, and 42.579 MMbbl more than the Kempers model. However, it underestimate GOIP by 22.137 Bft^3 less than the isothermal CG model, 36.935 Bft^3 less than the zero thermal diffusion CG model, 37.134 Bft^3 less than the Haase's thermal diffusion CG model, and 37.054 Bft^3 less than the Kempers thermal diffusion CG initialized reservoir model. These result has shown once again that neglecting compositional grading in reservoir simulator initialization has noteworthy technical consequences. Note that this inference method of comparing the performances of the various initialized reservoir simulation models was also applied by Jaramillo and Barrufet.[13] According to Favang et al.,[11] the essence of initializing reservoir simulation models adequately is not necessarily for improved fluid recovery but to ensure realistic and consistent reserves estimation and reservoir performances prediction for optimal field development economics.

Oil and Gas Production Rates. Figure 14 illustrates that the various initialized reservoir models exhibited similar constant oil production rate behavior from the start of production. However, the duration of the initial constant oil rate exhibited by the non-isothermal CG initialized reservoir models are shorter than the trends indicated by constant composition and isothermal CG initialized models, respectively. The longer constant oil rate exhibited by the constant composition initialized reservoir model could be attributed to the high OOIP estimated by the model, which is due to the constant composition (without CG) assumption. Consequently, the coupled fluid models are the most likely reasons for the observed differences in the predicted oil rate behavior of the various initialized reservoir models. This is because the coupled fluid models are the only variable in the various initialized reservoir model, otherwise, they should all indicate the same trends. The observed sharp drop in oil rates exhibited by the various initialized reservoir model after their initial constant rates suggests that due to poor permeability in some sections of the study reservoir, water injection is not the optimal pressure maintenance option for efficient development of the study reservoir.

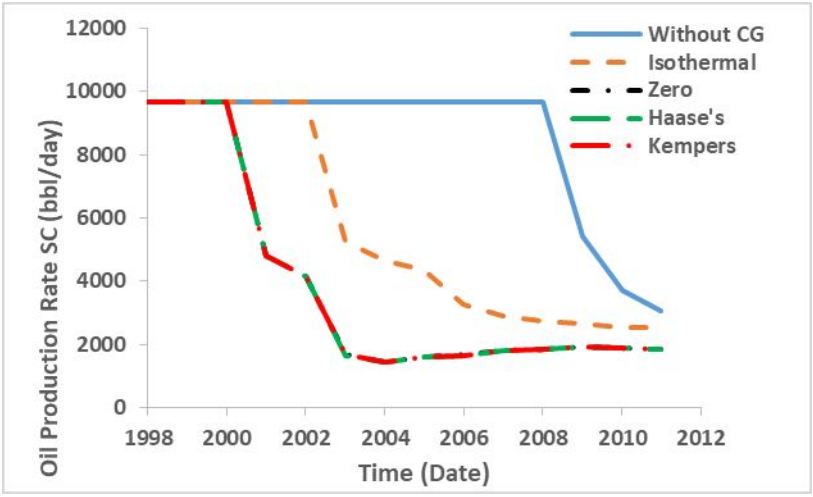

Figure 14. Oil Production Rates Predicted by the Various Initialized Reservoir Models under Water Injection

The simulated gas production rates for the various initialized reservoir models are shown in Figure 15. This figure shows that while the non-isothermal CG initialized reservoir model indicate suggestively similar trends, isothermal CG and constant composition initialized reservoir models exhibited different gas rate behaviors. The high gas rates simulated by the non-isothermal CG initialized models is a reflection of the high GOIP estimated by the various non-isothermal CG initialized reservoir models. Figure 15 also indicates that the constant composition initialized reservoir model, which estimated the least GOIP, also simulated the least initial gas rate (9.571693 $MMft^3$) and the highest ultimate gas rate of 12.008939 $MMft^3$.

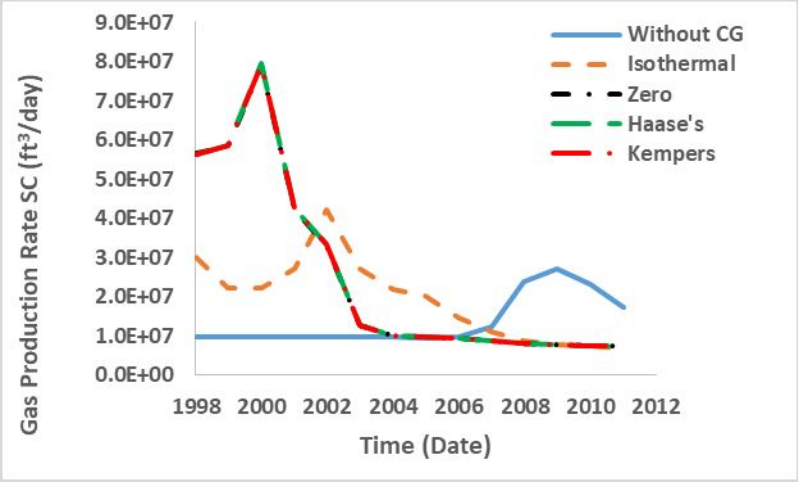

Figure 15. Gas Production Rates Predicted by the Various Initialized Reservoir Models under Water Injection

Cumulative Oil and Gas Produced. Predicted cumulative oil and gas produced by the various initialized reservoir simulation models are presented in Figures 16 and 17, respectively. Figure 16 shows that the models that neglected the effect of gravity and thermal diffusion (constant composition initialized reservoir model) predicted the highest ultimate cumulative oil, followed by isothermal CG initialized reservoir model, which accounted for the effect of gravity only. The high ultimate cumulative oil predicted by constant composition and isothermal CG initialized reservoir models are due to the high OOIP predicted by the two models. Figure 16 also shows

that models that accounted for the combined effect of gravity and temperature gradient or thermal diffusion (non-isothermal CG initialized reservoir models) predicted the least ultimate cumulative oil. There are no major difference in the cumulative oil trends exhibited by non-isothermal models as shown in Figure 16. Table 6 shows the ultimate cumulate oil simulated by the various initialized reservoir models.

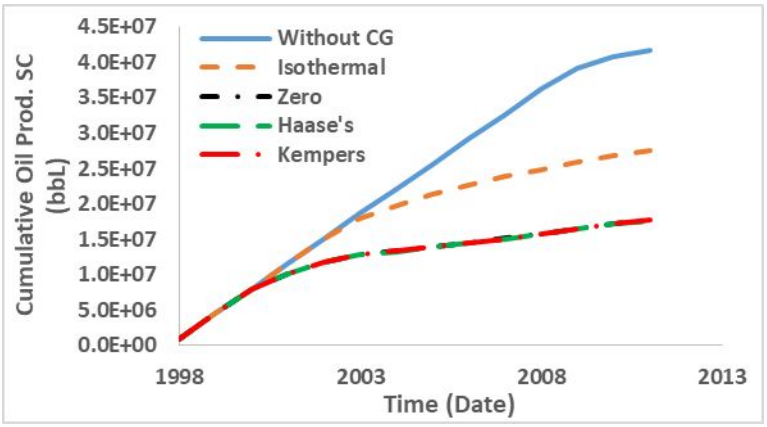

Figure 16. Cumulative Oil Produced versus Time, Predicted by Various Initialized Reservoir Models

Contrary to the trends observed in Figure 16, Figure 17 indicates that non-isothermal CG initialized reservoir models predicted high cumulative gas production relative to isothermal CG initialized reservoir model and constant composition initialized reservoir model. Therefore, for the study reservoir system, the combined effect of gravity and temperature gradient or thermal diffusion resulted in high gas production. Conversely, reservoir model initialized with the assumption of constant composition would result in low gas production. Figure 17 also illustrates that isothermal CG initialized reservoir model predicted higher cumulative gas than constant composition assumption but lower cumulative gas than non-isothermal model assumptions. The ultimate cumulative gas simulated by the various initialized reservoir models are summarized in Table 10.

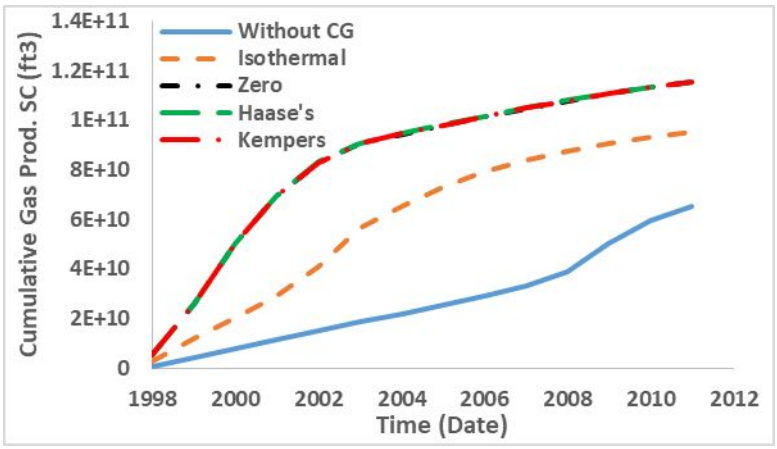

Figure 17. Cumulative Gas Produced versus Time, Predicted by Various Initialized Reservoir Models

Table 10. Ultimate Cumulative Oil and Gas Produced by the Various Initialized Reservoir Models

Models	Ultimate Cumulative Oil and Gas	
	Oil SC (MMbbl)	Gas SC (Bft^3)
Constant Composition	41.740	65.142
Isothermal	27.469	95.275
Zero Thermal Diffusion	17.693	115.456
Haase's	17.619	115.627
Kempers	17.652	115.550

Constant composition initialized reservoir model overestimate ultimate cumulative oil production by 14.271MMbbl more than the isothermal CG model, 24.047 MMbbl more than the zero thermal diffusion CG model, 24.120 MMbbl more than the Haase's thermal diffusion CG model, and 24.088 MMbbl more than the Kempers thermal diffusion CG model. It underestimated ultimate cumulative gas by 30.133 Bft^3 less than the isothermal CG, 50.314 Bft^3 less than the zero thermal diffusion CG model, 50.485 Bft^3 less than the Haase's thermal diffusion model, and 50.408 Bft^3 less than Kempers thermal diffusion CG initialized reservoir model. These differences are very noteworthy and should be a major technical concern and the major reason why CG should be adequately accounted for in the study reservoir. The ultimate

cumulative oil produced with isothermal CG initialized reservoir model is higher by 9.776 MMbbl than the zero thermal diffusion CG model, 9.850 MMbbl than the Haase's thermal diffusion CG model, and 9.817 MMbbl than the Kempers thermal diffusion CG initialized reservoir model. The ultimate cumulative gas produced with isothermal CG initialized reservoir model is lower by 20.181 Bft^3 than the zero thermal diffusion CG model, 20.352 Bft^3 than the Haase's thermal diffusion CG model, and 20.275 Bft^3 than the value indicated by Kempers thermal diffusion CG initialized reservoir model. Therefore, isothermal assumption for initialization of the study reservoir is grossly inadequate, since the results shows that thermal diffusion effect also contributed to the simulated CG.

The ultimate cumulative oil produced by zero thermal diffusion CG initialized reservoir model is greater by 73,430 bbl than the Haase's thermal diffusion CG model and 40, 784 bbl than the volume indicated by Kempers thermal diffusion CG initialized reservoir model. The ultimate cumulative gas produced by zero thermal diffusion CG initialized model is lower than the volume indicated by Haase's and Kempers thermal diffusion CG models by 171.049 $MMft^3$ and 94.110 $MMft^3$, respectively. Therefore, temperature gradient alone, without the corresponding thermal diffusion effect did not adequate describe compositional variation in the study reservoir. The ultimate cumulative oil difference between Haase's model (which assumed centre of mass for the calculation of thermal diffusion factor) and Kempers model (which assumed centre of volume for calculation of thermal diffusion factor) is 32,646 bbl while the ultimate cumulative gas difference is 76.939 $MMft^3$. Hence, center of mass assumption favors high oil production while center of volume assumption supports high gas production.

Gas-Oil Ratio. Gas-oil ratio (GOR) behaviors predicted by various initialized reservoir models are presented in Figure 18. The constant composition initialized reservoir model predicted the

lowest initial GOR and the highest ultimate producing GOR, followed by isothermal CG model, which however, indicated the lowest ultimate producing GOR. The non-isothermal models indicated the highest initial GOR but with ultimate GORs in between the values indicated by constant composition and isothermal models, respectively. The high GOR values exhibited by the non-isothermal models are clear reflection of their associated high cumulative gas production. There is no major difference in the predicted GOC behaviors exhibited by the non-isothermal models. Table 11 presents the values of the initial and ultimate GOR simulated by the different initialized reservoir models.

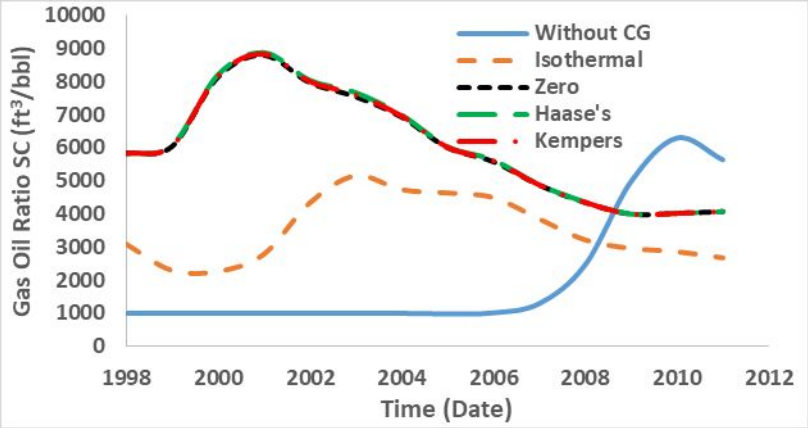

Figure 18. Gas Oil Ratio versus Time Predicted by Various Initialized Reservoir Models under Water Injection

Table 11. Initial and Ultimate GOR Predicted by the Different Initialized Reservoir Models under Water Injection

Models	GOR SC (ft^3/ bbl)	
	Initial	Ultimate
Constant Composition	997.044	5632.444
Isothermal	3103.399	2684.580
Zero Thermal Diffusion	5833.058	4061.564
Haase's	5808.893	4060.160
Kempers	5821.773	4061.277

Average Reservoir Pressure Profile. The average reservoir pressure behavior of the various initialized reservoir models, due to depletion and water injection, are illustrated in Figure 19. It shows that the pressure profile for the constant composition model increased steadily for about four years from start of production before declining throughout the simulation period. The pressure behavior for the isothermal model indicated declining rate with production, despite the influence of water injection. The reservoir pressure behavior of the non-isothermal CG initialized reservoir models indicated similar declining trends from start of production before increasing marginally from the year 2004 and throughout the remaining production period. The general behavior of the pressure profiles indicated by the various initialized reservoir model can be attributed to the amount of in-place fluid estimated by each model. Models that estimated high OOIP exhibited improved pressure profiles than those that estimated high GOIP volumes. The decline in average reservoir pressure exhibited by all the models, despite water injection, also demonstrates the limitations of water injection as the pressure maintenance option for the study reservoir.

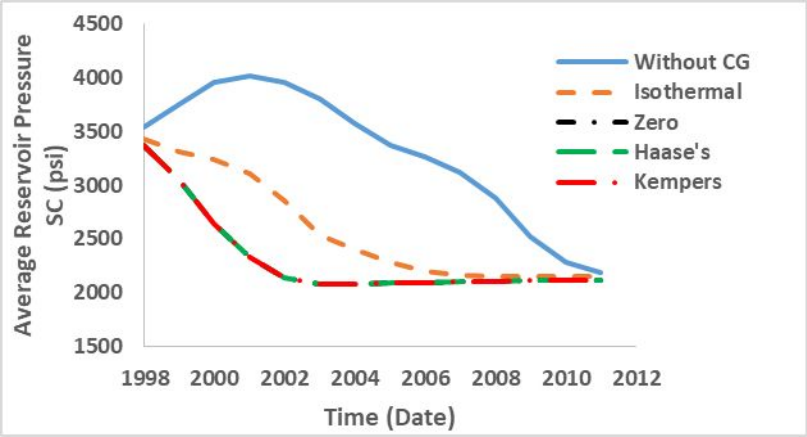

Figure 19. Average Reservoir Pressure Profile Predicted by Various Initialized Reservoir Models under Water Injection

3.3. Uncertainty Assessment

In the absence of historical production data for history matching, the range of uncertainties associated with estimated in-place volumes were quantified using Monte Carlo simulation (MCS) to predict the low case estimate (P10), best-case estimate (P50), and high case estimate (P90). The range of uncertainties indicated by the various initialized reservoir models (constant composition, isothermal CG, zero thermal diffusion CG, Haase's thermal diffusion CG, and Kempers thermal diffusion CG) are presented in this section. Obtained MCS results indicated the probability of non-exceedance curves for both OOIP and GOIP estimates for the different initialized reservoir models. The probability distribution curves are illustrated in Figures A1–A10 of the Supporting Information while the respective range of uncertainties are summarized in Tables 12 and 13 for OOIP and GOIP, respectively, which shows that the uncertainties associated with the OOIP and GOIP estimates for the different initialized reservoir models were successfully quantified.

Table 12. Range of Uncertainties Associated with the Estimated OOIP for the Various Initialized Reservoir Models

Models	Probabilistic OOIP SC (MMbbl)		
	P10	P50	P90
Constant Composition	161.508	174.342	187.275
Isothermal	139.466	150.602	161.740
Zero Thermal Diffusion	122.243	131.881	141.596
Haase's	121.969	131.792	141.560
Kempers	122.047	131.828	141.640

Table 13. Range of Uncertainties Associated with the Estimated GOIP for the Various Initialized Reservoir Models

Models	Probabilistic OOIP SC (Bft^3)		
	P10	P50	P90

Constant Composition	161.030	173.826	186.721
Isothermal	181.593	196.092	210.505
Zero Thermal Diffusion	195.377	210.781	226.308
Haase's	195.303	211.031	226.672
Kempers	195.283	210.933	226.635

The results of the UA also demonstrates that the regression model of the various initialized reservoir models are statistically significant. The 95 % confidence curves for both OOIP and GOIP for the various initialized reservoir response surface model verification plots illustrated in Figures B1–B10 of the Supporting Information, crossed their respective mean of responses. Figures B1–B10 shows that the proxy model predicted OOIP and GOIP for the different initialized reservoir models perfectly matched their initialized reservoir model simulated responses. The indicated training and verification experiments, which fall exactly on the 45-degree line, strongly confirmed that the created proxy models are valid proxies of the actual reservoir simulation responses. The experimental design qualities for the proxy models associated with the various reservoir models are within the orthogonal range (0–0.2) as shown in Table 14. Table 14 also shows that Kempers thermal diffusion CG initialized reservoir model indicated the lowest and most orthogonal design quality while constant composition initialized reservoir model generated the highest and less orthogonal design quality. Consequently, Table 14 suggests that Kempers thermal diffusion CG initialized reservoir model is the most realistic reservoir simulation model for the investigated reservoir system.

Table 14. Experimental Design Quality for the UA of the Various Initialized Reservoir Models

Models	**Orthogonality Value**
Constant Composition	0.039825
Isothermal	0.009438

Zero Thermal Diffusion	0.002283
Haase's	0.007107
Kempers	0.001607

3.4. Summary of Reservoir Model Validation

The various initialized reservoir models were validated based on the following procedures:

i. The deterministic reserve estimates were compared to the probabilistic estimates as shown in Tables 15 and 16 for OOIP and GOIP, respectively. Both Tables suggest no dramatic difference in the estimated in-place volumes, especially with respect to the base case estimates (P50). Hence, reservoir model assumptions and results are valid.

Table 15. Comparison of Probabilistic and Deterministic OOIP Estimates

Models	Probabilistic OOIP SC (MMbbl)			Deterministic SC OOIP (MMbbl)
	P10	P50	P90	
Constant Composition	161.508	174.342	187.275	174.428
Isothermal	139.466	150.602	161.740	150.569
Zero Thermal Diffusion	122.243	131.881	141.596	131.923
Haase's	121.969	131.792	141.560	131.802
Kempers	122.047	131.828	141.640	131.849

Table 16. Comparison of Probabilistic and Deterministic GOIP Estimates

Models	Probabilistic GOIP SC (Bft^3)			Deterministic GOIP SC (Bft^3)
	P10	P50	P90	
Constant Composition	161.030	173.826	186.721	173.913
Isothermal	181.593	196.092	210.505	196.050
Zero Thermal Diffusion	195.377	210.781	226.308	210.848
Haase's	195.303	211.031	226.672	211.047
Kempers	195.283	210.933	226.635	210.967

ii. The range of uncertainty associated with the estimated in-place volumes for the various initialized reservoir models were successfully quantified (see section 3.3, Tables 12 and 13).

iii. Response surface model verification plots for OOIP and GOIP associated with the various initialized reservoir models (presented in the Supporting information – Tables B1–B10) suggests that the regression models of the various initialized reservoir models are statistically significant at 0.05 probability. The 95 % confidence curves for both OOIP and GOIP crossed the mean of response in all cases. The model quality-check plots also indicates that the proxy model predictions perfectly matched the various initialized reservoir model results. The indicated training and verification experiments are exactly on the 45-degree line, which is an overwhelming indication that the created proxy models are valid proxies of the actual reservoir simulation responses. The summary of fit statistics for the various initialized reservoir models are presented in Tables 17 and 18 for OOIP and GOIP, respectively. The indicated R^2 values shows that the proxy models perfectly fits actual reservoir model results.

Table 17. Summary of Fit Statistics for OOIP

Model	R-Square	R-Square Adjusted	R-Square Predicted	Mean of Response	Standard Error
Constant Composition	1.0000	1.0000	1.0000	1.75337E+08	5.61056
Isothermal	1.0000	1.0000	1.0000	1.51353E+08	5.71830
Zero Thermal Diffusion	1.0000	1.0000	1.0000	1.31733E+08	4.40504
Haase's	1.0000	1.0000	1.0000	1.31589E+08	4.19402
Kempers	1.0000	1.0000	1.0000	1.31751E+08	4.07718

Table 18. Summary of Fit Statistics for GOIP

Models	R-Square	R-Square Adjusted	R-Square Predicted	Mean of Response	Standard Error
Constant Composition	1.0000	1.0000	1.0000	1.74819E+11	6059.60

Isothermal	1.0000	1.0000	1.0000	1.97070E+11	6477.76
Zero Thermal Diffusion	1.0000	1.0000	1.0000	2.10544E+11	7243.01
Haase's	1.0000	1.0000	1.0000	2.10706E+11	7282.15
Kempers	1.0000	1.0000	1.0000	2.10811E+11	7244.35

iv. The experimental design quality for proxy models of the initialized reservoir models are within the orthogonal range (0–0.2). Hence, model assumptions and results are valid.

4. CONCLUSIONS

Neglecting CG or inadequate account of CG effects in reservoir simulation model initialization resulted in overestimation of OOIP and underestimation of GOIP. The constant composition (without CG) initialized reservoir model inevitably overestimated the OOIP and underestimate the GOIP. It also overestimate ultimate cumulative oil production by 14.271 MMbbl more than the isothermal CG model, 24.047 MMbbl more than zero the thermal diffusion CG model, 24.120 MMbbl more than the Haase's thermal diffusion CG model, and 24.088 MMbbl more than the Kempers thermal diffusion CG model. It underestimated ultimate cumulative gas by 30.133 Bft^3 less than isothermal CG, 50.314 Bft^3 less than the zero thermal diffusion CG model, 50.485 Bft^3 less than the Haase's thermal diffusion model, and 50.408 Bft^3 less than the Kempers thermal diffusion CG initialized reservoir model.

Therefore, any technical decision made based on production forecast derived from models that ignored or inadequately accounted for compositional grading effects, will inevitably lead to detrimental technical consequences. For instance, field development decisions based on the performances of constant composition or isothermal CG initialized reservoir models, will lead to wasted investment in the design and procurement of oversized surface and subsurface oil production handling facilities and equipment. Both models significantly overestimated oil production. Such development decision will also mean the design or procurement of undersized

surface handling facilities for gas production since constant composition and isothermal CG initialized reservoir models grossly underestimated cumulative gas production. This could lead to more adverse technical consequences such as loses in production or complete operational shutdown due to limited surface handling capacity for the unexpected high volume of produced gas. It could also lead to environment issues such as gas flaring.

SUPPORTING INFORMATION

Supporting Information is available free of charge via the Internet at http://pubs.acs.org.

Figure A1: OOIP Probability Distribution Estimated by Constant Composition Initialized Reservoir Model;

Figure A2: GOIP Probability Distribution Estimated by Constant Composition Initialized Reservoir Model;

Figure A3: OOIP Probability Distribution Estimated by Isothermal CG Initialized Reservoir Model;

Figure A4: GOIP Probability Distribution Estimated by Isothermal CG Initialized Reservoir Model;

Figure A5: OOIP Probability Distribution Estimated by Zero Thermal Diffusion CG Initialized Reservoir Model;

Figure A6: GOIP Probability Distribution Estimated by Zero Thermal Diffusion CG Initialized Reservoir Model;

Figure A7: OOIP Probability Distribution Estimated by Haase's Thermal Diffusion CG Initialized Reservoir Model;

Figure A8: GOIP Probability Distribution Estimated by Haase's Thermal Diffusion CG Initialied Reservoir Model;

Figure A9: OOIP Probability Distribution Estimated by Kempers Thermal Diffusion CG Initialized Reservoir Model;

Figure A10: GOIP Probability Distribution Estimated by Kempers Thermal Diffusion CG Initialized Reservoir Model;

Figure B1: OOIP Response Surface Model Verification Plot for Constant Composition Initialized Reservoir Model;

Figure B2: GOIP Response Surface Model Verification Plot for Constant Composition Initialized Reservoir Model;

Figure B3: OOIP Response Surface Model Verification Plot for Isothermal CG Initialized Reservoir Model;

Figure B4: GOIP Response Surface Model Verification Plot for Isothermal CG Initialized Reservoir Model;

Figure B5: OOIP Response Surface Model Verification Plot for Zero Thermal Diffusion CG Initialized Reservoir Model;

Figure B6: GOIP Response Surface Model Verification Plot for Zero Thermal Diffusion CG Initialized Reservoir Model;

Figure B7: OOIP Response Surface Model Verification Plot for Haase's Thermal Diffusion CG Initialized Reservoir Model;

Figure B8: GOIP Response Surface Model Verification Plot for Haase's Thermal Diffusion CG Initialized Reservoir Model;

Figure B9: OOIP Response Surface Model Verification Plot for Kempers Thermal Diffusion CG Initialized Reservoir Model;

Figure B10: GOIP Response Surface Model Verification Plot for Kempers Thermal Diffusion CG Initialized Reservoir Model.

CORRESPONDING AUTHOR

*Jebraeel Gholinezhad (jebraeel.gholinezhad@port.ac.uk), School of Energy and Electronic Engineering, Anglesea Building, University of Portsmouth, PO1 3DJ, United Kingdom.

Tel: +44 2392 8423 41.

ORCID

Ikechi Igwe: 0000-0002-9298-8305

Jebraeel Gholinezhad: 0000-0002-0495-9812

AUTHOR CONTRIBUTIONS

The manuscript was written through contributions of all authors. All authors have given approval to the final version of the manuscript. These authors, Ikechi Igwe, Jebraeel Gholinezhad, Mohamed Galal Hassan Sayed, and Frank Ogbuagu, contributed equally to editing the manuscript.

FUNDING

This study was supported financially by Tertiary Education Trust Fund (TETFund) of Nigeria under the Academic Staff Training and Development award (2014/2015).

DISCLOSURE STATEMENT

There is no conflict of interest to declare.

ACKNOWLEDGEMENT

The authors wish to sincerely thank the anonymous reviewers and the editor whose corrections and comments have significantly enhanced the quality of this manuscript.

REFERENCES

(1) Ezekwe, N. *Petroleum Reservoir Engineering Practice*; Pearson Education/Prentice Hall: Boston, Massachusetts, 2011; pp 681–707.

(2) Hamoodi, A. N.; Abed, A. F.; Grabenstetter, J. Modeling of a large gas- capped reservoir with areal and vertical variation in composition. SPE Annual Technical Conference and Exhibition, New Orleans, Louisiana, Sept 25–28, 1994.

(3) Høier, L.; Whitson, C. H. Compositional grading-theory and practice. SPE Annual Technical Conference and Exhibition, Dallas, Texas, Oct 1–4, 2000.

(4) Leahy-Dios, A. Experimental and theoretical investigation of Fickian and thermal diffusion coefficients in hydrocarbon mixtures. Ph.D. Thesis, Yale University, May 2008.

(5) Bogatyrev, A. F.; Makeenkova, O. A.; Nezovitina, M. A. Experimental study of thermal diffusion in multicomponent gaseous systems. *International Journal of Thermophysics* **2015**, *36*, 633–647.

(6) Nikpoor, M. H.; Kharrat, R.; Chen, Z. Non-isothermal modeling of compositional grading in petroleum reservoirs, including the effect of plus fraction properties changes with depth. *Pet. Sci. Technol*. **2011**, *29*, 914–923.

(7) Nikpoor, M. H.; Kharrat, R.; Chen, Z. The modeling of 3D compositional grading and plus fraction molecular weight change in non-isothermal petroleum reservoirs. *Energy Sources, Part A: Recovery, Utilization, and Environmental Effects* **2013**, *35*, 99–109.

(8) Nikpoor, M. H.; Dejam, M.; Chen, Z.; Clarke, M. Chemical–Gravity–Thermal Diffusion Equilibrium in Two-Phase Non-isothermal Petroleum Reservoirs. *Energy Fuels* **2016**, *30*, 2021–2034.

(9) Pedersen, K. S.; Hjermstad, H. P. Modeling of Compositional Variation with Depth for Five North Sea Reservoirs, SPE Annual Technical Conference and Exhibition, Houston, Texas, U.S.A, Sept 28–30, 2015.

(10) Whitson, C. H.; Belery, P. Compositional gradients in petroleum reservoirs, University of Tulsa Centennial Petroleum Engineering Symposium, Tulsa, Oklahoma, Aug 29–31, 1994.

(11) Fevang, Ø.; Singh, K.; Whitson, C. H. Guidelines for choosing compositional and black-oil models for volatile oil and gas-condensate reservoirs, SPE Annual Technical Conference and Exhibition, Dallas, Texas, Oct 1–4, 2000.

(12) Whitson, C. H.; Fevang, Ø.; Yang, T. Gas Condensate PVT: What's Really Important and Why? IBC Conference on Optimization of Gas Condensate Fields, London, Jan 28-29, 1999.

(13) Jaramillo, J. M.; Barrufet, M. A. Effects in the determination of oil reserves due to gravitational compositional gradients in near-critical reservoirs, SPE Annual Technical Conference and Exhibition, New Orleans, Louisiana, Sept 30–Oct 3, 2001.

(14) Liu, J. S.; Wilkins, J. R.; Al-Qahtani, M. Y.; Al-Awami, A. A. Modeling a rich gas condensate reservoir with composition grading and faults, SPE Middle East Oil Show, Manama, Bahrain, Mar 17–20, 2001.

(15) Luo, S.; Barrufet, M. A. Compositional gradient: its role in near-critical reservoir development. *Journal of Petroleum Science and Engineering* **2004,** *45*, 193–201.

(16) Vo, H. X.; Horne, R. N. Experimental Study of Composition Variation During Flow of Gas-Condensate, SPE Annual Technical Conference and Exhibition, Houston, Texas, U.S.A., Sept 28–30, 2015.

(17) Mokhtari, R.; Ashouri, S. Importance of compositional grading in reservoir development studies: a case study. *Sci. Int. (Lahore)* **2013**, *25*, 457–462.

(18) Høier, L. Miscibility Variations in Compositionally Grading Petroleum Reservoirs. Ph.D. Thesis, Norwegian University of Science and Technology, NTNU, November 1997.

(19) Montel, F.; Gouel, P. L. Prediction of compositional grading in a reservoir fluid column, SPE Annual Technical Conference and Exhibition, Las Vegas, Nevada, Sept 22–26, 1985.

(20) Montel, F. Phase equilibria needs for petroleum exploration and production industry. *Fluid Phase Equilibria* **1993**, *84*, 343–367.

(21) Faissat, B.; Knudsen, K.; Stenby, E. H.; Montel, F. Fundamental statements about thermal diffusion for a multicomponent mixture in a porous medium. *Fluid Phase Equilibria* **1994**, *100*, 209–222.

(22) Igwe, I.; Gholinezhad, J.; Hassan, M. The effect of equations of state on the performances of compositional grading models. *Energy Sources, Part A: Recovery, Utilization, and Environmental Effects* **2019**, 1–13.

(23) Haase, R. Thermodynamics of irreversible processes; Addison-Wesley: New York, 1969, Chapter 4.

(24) Kempers, L. J. A thermodynamic theory of the Soret effect in a multicomponent liquid. *The Journal of Chemical Physics* **1989** *90*, 6541–6548.

(25) Sage, B. H.; Lacey, W. N. Gravitational concentration gradients in static columns of hydrocarbon fluids. *Transactions of the AIME* **1939**, *132*, 120–131.

(26) Schulte, A. M. Compositional variations within a hydrocarbon column due to gravity, SPE Annual Technical Conference and Exhibition, Dallas, Texas, Sept 21–24, 1980.

(27) Whitson, C. H.; Belery, P. Compositional gradients in petroleum reservoirs. University of Tulsa Centennial Petroleum Engineering Symposium, Tulsa, Oklahoma. Aug 29–31, 1994.

(28) Boukadi, F.; Bemani, A.; Rumhy, M. Effect of PVT properties variation with depth in hydrocarbon reservoirs. *Petroleum Science and Technology* **1999**, 17, 81–98.

(29) Esposito, R. O.; Alijó, P. H. R.; Scilipoti, J. A.; Tavares, F. W. Compositional grading in Oil and Gas reservoirs. Gulf Professional Publishing, 2017, pp 35–217.

(30) Galliero, G.; Bataller, H.; Bazile, J. P.; Diaz, J.; Croccolo, F.; Hoang, H.; Bou-Ali, M. M. Thermodiffusion in multicomponent n-alkane mixtures. *npj Microgravity* **2017**, *3*, 20.

(31) Dougherty Jr, E. L.; Drickamer, H. G. Thermal diffusion and molecular motion in liquids. *The Journal of Physical Chemistry* **1955**, *59*, 443–449.

(32) Belery, P.; Da Silva, F. V. Gravity and thermal diffusion in hydrocarbon reservoirs. Third Chalk Research Program, Jun 11–12, 1990.

(33) Shukla, K.; Firoozabadi, A. A new model of thermal diffusion coefficients in binary hydrocarbon mixtures. *Industrial & engineering chemistry research* **1998**, *37*, 3331–3342.

(34) Jacqmin, D. The interaction of natural convection and gravity segregation in oil/gas reservoirs, SPE Annual Technical Conference and Exhibition, Dallas, Texas, Sep 27–30, 1987.

(35) Firoozabadi, A.; Ghorayeb, K.; Shukla, K. Theoretical Model of Thermal Diffusion Factors in Multicomponent Mixtures. *AIChE Journal* **2004,** *46*, 892–900.

(36) Moser, R. D. Mass transfer by thermal convection and diffusion in porous media, 10th International Conference on Applied Mathematics, Austin, Texas, Jun 1986.

(37) Riley, M. F.; Firoozabadi, A. Compositional variation in hydrocarbon reservoirs with natural convection and diffusion. *AIChE journal* **1998,** *44*, 452–464.

(38) Ghorayeb, K.; Firoozabadi, A. Numerical study of natural convection and diffusion in fractured porous media. *SPE Journal* **2000,** *5*, 12–20.

(39) Ghorayeb, K.; Firoozabadi, A. Features of convection and diffusion in porous media for binary systems. *Journal of Canadian Petroleum Technology* **2006,** *40*, 21–28.

(40) Nasrabadi, H.; Ghorayeb, K.; Firoozabadi, A. Two-phase multicomponent diffusion and convection for reservoir initialization. *SPE Reservoir Evaluation & Engineering* **2006**, *9*, 530–542.

(41) Montel, F.; Hoang, H.; Galliero, G. (2019). Linking up pressure, chemical potential and thermal gradients. *The European Physical Journal E* **2019,** *42,* 1–10

(42) Pedersen, K. S.; Lindeloff, N. Simulations of compositional gradients in hydrocarbon reservoirs under the influence of a temperature gradient. SPE Annual Technical Conference and Exhibition, Denver, Colorado, Oct 5–8, 2003.

(43) Pedersen, K. S.; Hjermstad, H. P. Modeling of large hydrocarbon compositional gradient. Abu Dhabi International Petroleum Exhibition and Conference, Abu Dhabi, UAE, Nov 5-8, 2006.

(44) Ghorayeb, K.; Firoozabadi, A.; Anraku, T. Interpretation of the unusual fluid distribution in the Yufutsu gas-condensate field. *SPE journal* **2003**, *8*, 114–123.

(45) Agarwal, R.; Li, Y. K.; Nghiem, L. A regression technique with dynamic-parameter selection or phase behavior matching. SPE California Regional Meeting, Ventura, California, Apr 8–10, 1987.

(46) Jordi Vilanova Linkedin Page. https://www.linkedin.com/pulse/comparison-deterministic-probabilistic-methods-improve-jordi-vilanova (accessed Aug 3, 2019).

(47) SPE/WPC/AAPG/SPEE/SEG/SPWLA/EAGE. Petroleum Resources Management System. https://www.spe.org/industry/docs/Petroleum-Resources-Management-System.pdf?ecid=O~E~~~B2B~Listed@ASX~~201711~4D17FF62DA924A448FCAEF04CEC4541A~ (accessed Jul 4, 2019).

(48) CMOST Manual. Intelligent Optimization and Analysis Tool, Computer Modelling Group LTD, 2017.

(49) Sall, J. Leverage plots for general linear hypotheses. *The American Statistician* **1990**, *44*, 308–315.